Design and Characterization of a High sensitivity 2.45 GHz E-Field Probe for Precise Electromagnetic Measurements

Abhinav Mishra[1,3*], N.P Singh[2], A.K Katiyar[1], and S.K Dubey[1]
[1]CSIR-National Physical Laboratory, New Delhi-110012, India
[2]Gurukul kangri Vishwavidyalaya, Haridwar, Uttarakhand-249404, India
[3]Government Polytechnic Gopalganj, Bihar 841501, India

Corresponding author: Abhinav Mishra (e-mail: mishra.abhinav162@gmail.com).

ABSTRACT This work presents the design, simulation, and experimental validation of a novel electric-field (E-field) probe operating at 2.45 GHz, developed specifically for electromagnetic field measurements and calibration applications. The proposed probe incorporates a compact cylindrical dipole architecture, enhanced with a low-loss Teflon dielectric spacer to ensure structural stability and minimal field disturbance. A high-speed Schottky diode rectification circuit is employed to enable efficient detection of weak electric fields while maintaining a reliable response over the operating bandwidth. The resulting probe achieves good impedance matching, with $S_{11} < -16$ dB at 2.45 GHz, and offers a usable bandwidth of approximately 100 MHz around the target frequency. Performance evaluation demonstrates high sensitivity (10 mV/m), strong linearity ($R^2 = 0.996$), and low measurement uncertainty (±2.8 dB). When compared with widely used commercial probes, such as the NARDA NBM-50, the developed design exhibits comparable performance in terms of sensitivity and stability, making it suitable for EMC and dosimetry applications.

INDEX TERMS Dipole probe, E-Field Sensor, Gigahertz TEM cell, vector network analyzer.

I. INTRODUCTION

Accurate measurement of the electric field is crucial in a wide range of scientific and engineering applications, including electromagnetic interference/electromagnetic compatibility (EMI/EMC) compliance testing, and other medical application [1-4]. Assessment of such fields requires highly accurate and reliable measuring devices such as E-Field sensors, probes, and electromagnetic field (EMF) testers. These devices need calibration with reference standards at regular intervals to maintain measurement accuracy and precision. The devices are calibrated by a standard Electric field generation system [5-7]. The introduction of electric field probes for calibration has significantly advanced measurement precision in both laboratory and field applications. In the beginning era, research emphasized enhancing probe sensitivity and dynamic range, with pioneering work by Schmid et al. highlighting the need for high-frequency response in electromagnetic fields [8]. Innovations continued through as active and passive probes were refined. The development of fiber-optic techniques by H. Takahashi et al. showcased reduced perturbation effects on electromagnetic fields [9]. The turn of the millennium witnessed further breakthroughs with the advent of nano-technologies enhancing spatial resolution (Müller et al) [10]. In the recent, advancements have focused on integrating digital signal processing into probe design to improve accuracy and ease of use [11]. These developments underscore a sustained commitment to advancing electric field measurement methodologies which remain crucial for compliance testing and research across various scientific domains [12]. With recent advancements in RF and microwave technology, the importance of E-field sensing has significantly increased. Electric field measurement techniques involve using various sensors and methods to quantify the strength and direction of electric fields [13-16]. These techniques range from simple contact measurements using high-impedance preamplifiers to more sophisticated non-contact methods like optical sensors and field mills. Traditional techniques like Faraday pails and electric field mills have limitations and require meticulous calibration and integration with specific industrial processes. As industries such as telecommunications, automotive, and medical demand more precise and reliable data, Proper calibration and validation of measurement systems are essential for ensuring the accuracy and reliability of the results [17]. the development of E-field sensors/probes has filled a significant gap in the market. In this work, details the design and development of a novel E-field sensor that provides precise, reliable, and versatile measurement capabilities. This cost-effective sensor plays a critical role in advancing electromagnetic field measurement technology by offering precise E-field measurements. The Electric field produced by the generation system was further validated against a standard E-Field probe. Also, the measured results

with the E-Field sensor were compared with a commercially available probes/sensors.

II. E-FIELD PROBE DESIGN

The proposed dipole antenna cylindrical design at HFSS simulator to operate at 2.45 GHz resonant frequency fr on Teflon material substrate and L"$_{eff}$" is effective length of the dipole (m), ε"$_{eff}$" is effective dielectric constant of the medium. Teflon circular material having 2 cm diameter sandwich between two brass material cylindrical shape having each length of 2.5cm with 0.2cm separation between them with Teflon material. In probe design we connect a Schottky diode between brass rod and two resistors of 100kΩ and one capacitor of 500 pf to rectify the induced RF voltage and give coaxial feed using SMA connector. For a half-wave dipole antenna resonant frequency [18]:

$$f_r = \frac{c}{2L_{\text{eff}}\sqrt{\varepsilon_{\text{eff}}}} \quad (1)$$

If the dipole is implemented over a dielectric or microstrip substrate, the effective permittivity is approximated as:

$$\varepsilon_{\text{eff}} = \frac{\varepsilon_r+1}{2} + \frac{\varepsilon_r-1}{2}\left(1+12\frac{h}{W}\right)^{-1/2} \quad (2)$$

where, ε_r is relative permittivity of substrate (for Teflon, 2.2), h is substrate height (m), W is conductor width (m). The primary dimensions of the E-field probe can be calculated and tabulated in the below table1.the geometrical configuration of proposed electric field probe and its fabricated design is shown in figure1 and 2 respectively.

TABLE I. Electric field probe geometrical parameter.

Symbol	Parameters	Value
L_1	Brass rod length	2.5 cm
g	Dielectric thickness	0.2 cm
D	Dielectric diameter	2.0 cm
L_t	Antenna length	5.2 cm
R_1, R_2	Resistors	100 kΩ
C_1	Capacitor	500 pF

III. MEASUREMENT SETUP

Measurement of the reflection coefficient (S_{11}) using a Vector Network Analyzer (VNA) requires careful procedures to ensure accurate results. The VNA is first calibrated according to the manufacturer's guidelines, with particular attention to cable and adapter configurations. The device under test (DUT) is then connected to the VNA using high-quality test cables to minimize interference and signal loss. The measurement frequency range and bandwidth are set in accordance with the specifications of the DUT. Multiple measurements are taken across the frequency range to obtain comprehensive data for analysis. The measured S_{11} values are then analyzed to evaluate impedance matching and signal reflection characteristics. The measurement setup for S_{11} is shown in Figure 3. The electric field measurements were conducted inside a GTEM cell under controlled conditions. A signal generator was used to excite the system at 2.45 GHz, and the input RF power was varied systematically to generate different electric field strengths. The proposed E-field probe was placed at a fixed distance from the source and aligned along the direction of the electric field polarization to ensure maximum response. Care was taken to minimize reflections and external interference during measurements. Calibration of the E-field probe was performed using a reference probe to establish a relationship between the input RF power and the corresponding electric field strength. The reference probe (NARDA) used for benchmarking. Calibration curves were generated by recording the probe output response for known electric field values. These curves were then used to convert measured output signals into actual electric field strength (V/m). The linearity and sensitivity of the electromagnetic (EM) sensor were evaluated within a GTEM cell. Sensitivity, defined as the minimum detectable electric field strength, and linearity, determined from the logarithmic relationship between input power and output response, were the key parameters investigated. The linearity response of the probe was assessed during the calibration process. The E-field

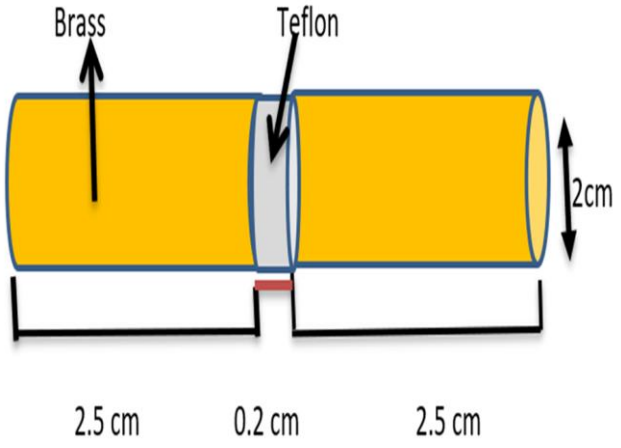

FIGURE 1. Schematic diagram of simulated Electric field probe.

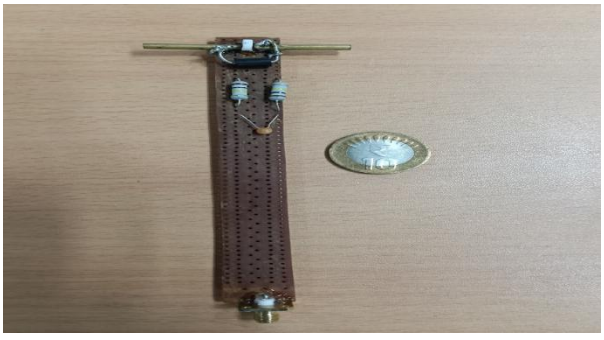

FIGURE 2. developed design of fabricated Electric field probe.

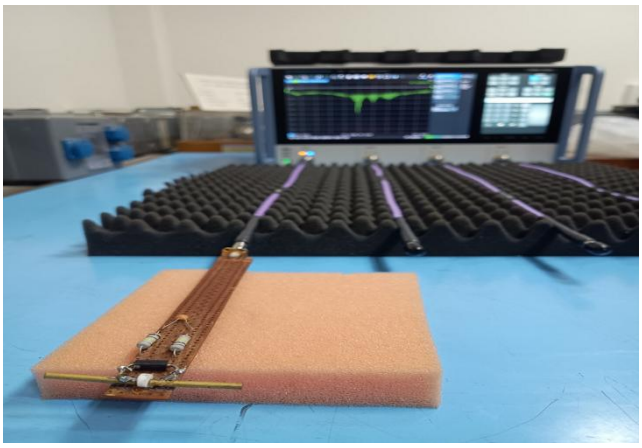

FIGURE 3. Measurement setup of Reflection coefficient of Proposed E-Field Probe.

IV. RESULTS AND DISCUSSION

The result section first discusses simulation result of reflection coefficient of E-Field probe design and the other part discuss the E-field characterizing parameter sensitivity, linearity and the uncertainty budget The experimental results obtained are shown in Figure 5. Figure 4 illustrates the simulated return loss (S_{11}) characteristics of the proposed cylindrical dipole antenna designed to operate at 2.45 GHz. the antenna exhibits a distinct resonance at approximately 2.45 GHz, where the S_{11} curve reaches its minimum value of about –16 dB and 100 MHz bandwidth.

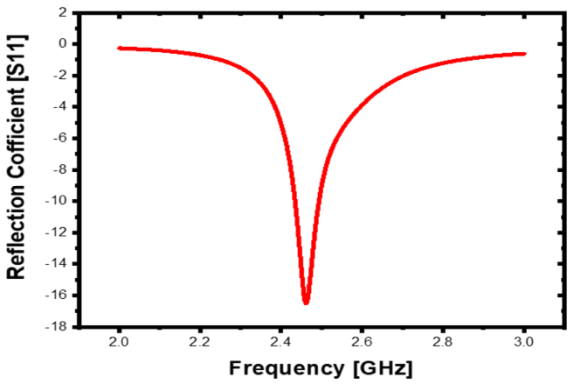

FIGURE 4. Reflection coefficient of Proposed E-Field Probe sensor.

The high-quality impedance matching is achieved through careful optimization of the dipole dimensions, the dielectric Teflon spacer, and the brass element geometry. This ensures consistent and reliable performance in practical measurement and sensing environments. Figure 5 presents the measured relationship between the input RF power level (dBm) and the corresponding induced electric field strength (mV/m) for both the proposed probe and a standard NARDA reference probe. The experiment was conducted at the resonant frequency of 2.45 GHz, and the applied RF power was varied from –30 dBm to 0 dBm to evaluate the probe's linearity and sensitivity characteristics. The proposed probe (black line) demonstrates a very close correlation with the NARDA probe (red line) across the entire power range, indicating that the developed sensor is capable of accurately replicating the performance of the commercial reference device. At lower power levels (below –20 dBm), the proposed probe shows slightly higher field sensitivity, producing marginally higher output values compared to the NARDA probe. This improvement can be attributed to the optimized cylindrical geometry and low-loss Teflon dielectric that enhance the local field concentration around the sensing gap, thereby increasing the rectified voltage from the Schottky diode. At higher power levels (above –10 dBm), both probes converge, showing nearly identical responses up to the maximum applied power of 0 dBm. This demonstrates that the proposed design maintains good linearity and stability over a wide dynamic range of incident RF power.

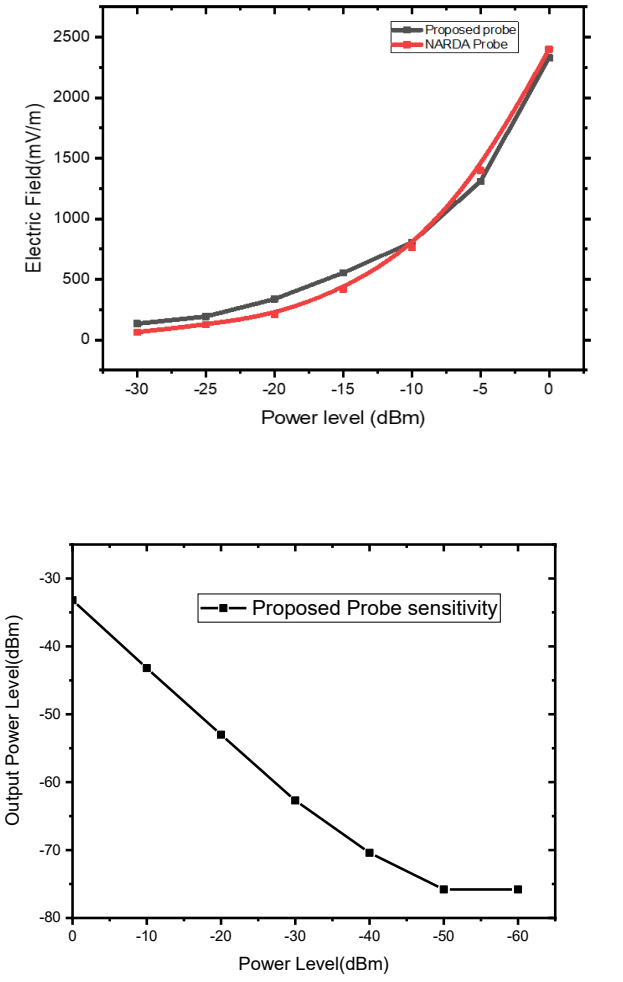

FIGURE 5. Linearity and sensitivity of Proposed E-Field Probe sensor and NBM-NARDA 50.

Analysis of the proposed E-field probe indicates that the sensor achieves high sensitivity (10 mV/m), good linearity (R^2 = 0.996), and field uniformity within ± 2.8 dB, demonstrating compliance with IEC 61000-4-20. The combination of optimized cylindrical dipole geometry and low-loss Teflon dielectric contributes to the improved response at low input levels compared to the commercial NARDA probe. New insights point to log RF power detectors, where the dynamic range covers inputs like 0 to -60 dBm with linear output in dB scale. The sensitivity drops steadily as the input power decreases, with a noticeable levelling off below -60 dBm, where the electric field strength stabilizes around 10 mV/m. Maximum gain value achieved approximately -5 dB simulated which validate through measured data near the resonance frequency shown in figure 6, indicating the device's best performance point.

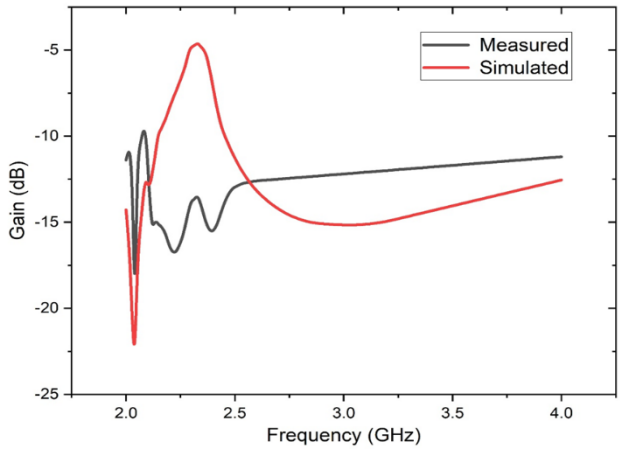

FIGURE 6. Simulated and measured Gain of Proposed E-Field Probe sensor.

V. UNCERTAINTY ANALYSIS

The uncertainty budget estimated for the theoretical electric field (16 V/m) at 2.45 GHz is provided in Table 3. Errors in measuring position, attenuation, power level, SWR, and resistance measurement contribute significantly to the overall uncertainty budget. The expanded uncertainty (k = 2) obtained is 5.41% at a field strength of 16 V/m. Similarly, Table 2 presents the uncertainty values obtained for the measured electric field (16.30 V/m) at 2.45 GHz. The primary sources of uncertainty are associated with the power level, SWR, and resistance measurement. Furthermore, the expanded uncertainties for the generation system at 2.45 GHz are presented in Table 3. The expanded uncertainty (k = 2) obtained is 5.23% at a field strength of 16.30 V/m.

FIGURE 7. Calibration and measurement setup of E-field (a) developed probe (b) standard reference probe NBM-50.

TABLE II. Uncertainty budget for Measured Electric field, 16.30 V/m at 2.45 GHz.

Sources of Uncertainty	Symbol	Standard Uncertainty	Type/Probability Distribution	Sensitivity Coefficient	Uncertainties (V/m)	Uncertainties (%)
UA Repeatability	u_1	0.00374	A/t	1	0.003742	0.0230
UB1 (Atten.)	u_2	0.001	B/Normal	10	0.01	0.0613
UB2 (Power)	u_3	0.0001	B/Normal	4000	0.4	2.4540
UB3 (Position)	u_4	0.0005	B/Normal	250	0.125	0.7663
UB4 (SWR)	u_5	0.01556	B/U	5	0.077793	0.4772
UB5(Meter Res)	u_6	0.00289	B/Rectangular	1	0.002887	0.0177
Combined Uncertainty, $u_c = \sqrt{(u_1^2 + u_2^2 + u_3^2 + u_4^2 + u_5^2)}$						**0.426379**
Expanded Uncertainty (at k = 2)						**.8528**

TABLE III. Uncertainty budget for Theoretical Electric field, 16 V/m at 2.45 GHz.

Sources of Uncertainty	Symbol	Standard Uncertainty	Type/Probability Distribution	Sensitivity Coefficient	Uncertainties (V/m)	Uncertainties (%)
UA Repeatability	u_1	0	A/t	1	0	0.000
UB1 (Atten.)	u_2	0.001	B/Normal	2	0.002	0.0125
UB2 (Power)	u_3	0.0001	B/Normal	1250	0.125	0.7813
UB3 (Position)	u_4	0.0005	B/Normal	50	0.025	0.1563
UB4 (SWR)	u_5	0.0332 4	B/U	5	0.1662	1.0388
UB5 (Meter Res)	u_6	0.0028 9	B/Rectangular	1	0.00289	0.0181
Combined Uncertainty, $u_c = \sqrt{(u_1^2 + u_2^2 + u_3^2 + u_4^2 + u_5^2 + u_6^2)}$						**0.4325**
Expanded Uncertainty (at $k = 2$)						-

COMPARISON WITH SIMILAR SYSTEMS

Comparison of developed E-Field field generation setup with some of the similar systems available in literature have been provided in Table 4. These systems have been developed targeted to specific applications and have their own pros and cons. Design E-Field probe delivers superior low level sensitivity and an excellent dynamic/linear range, positioning it favorably against leading market probes. In this work, the system has been designed covering wide range of frequencies with good linearity with sensitivity range.

TABLE IV. Comparison of developed E-Field field generation setup with some of the similar systems.

Probe Model	Min. Sensitivity (E-field)	Frequency Range	Dynamic Range	Linearity Range	Return Loss / Matching
Proposed Probe	**10 mV/m** (@ – 80 dBm)	~2.45 GHz design	~80 dB	0 dBm to –50 dBm	S11 < – 16 dB at 2.45 GHz
Narda EP-600	10 mV/m (@ ≤–70 dBm)	100 kHz–9.25 GHz	80 dB	0 dBm to –40 dBm	< –15 dB typical
Narda EA 5091	0.5 V/m (≙500 mV/m)	300 kHz–50 GHz	30 dB	–10 dBm to +10 dBm	–10 dB to –20 dB
Narda EP-602	1.5 V/m (≙1500 mV/m)	5 kHz–9.25 GHz	60 dB	0 dBm to –50 dBm	< –12 dB
Narda EF 0392	1300 V/m	100 kHz–3 GHz	~60 dB	–10 dBm to +10 dBm	N/A (shaped probe)

VI. CONCLUSION

A novel and cost-effective electric field (E-field) sensor has been developed and experimentally demonstrated for reliable field measurements. The proposed sensor design combines affordability with high sensitivity, ensuring consistent performance across a range of applications. The sensor is specifically optimized to operate at 2.45 GHz, a widely used ISM band frequency, and the experimental results show good agreement with the designed resonant characteristics at this frequency. Through experimental validation and comparative analysis with a standard probe, the sensor exhibits good linearity and sensitivity while maintaining low operational cost. At 2.45 GHz, the measured performance parameters, including reflection coefficient, sensitivity, and uncertainty, demonstrate that the proposed sensor provides stable and consistent response suitable for practical measurement scenarios. Its compact size and cost-effectiveness make it suitable for both laboratory and field environments. The developed dipole-based E-field sensor has potential applications in biomedical diagnostics, such as monitoring electric field levels in therapeutic systems; electromagnetic interference and Electromagnetic Compatibility (EMI/EMC) compliance testing of electronic instruments; and industrial monitoring applications, including RF and microwave systems.

ACKNOWLEDGMENT

The authors would like to thank Ms. Prachi Tyagi, Sr. Research Scholar, Electromagnetic Metrology Section, CSIR-NPL, New Delhi for providing technical support for this research work. All the financial support for this work was provided by Director, CSIR-NPL, New Delhi.

REFERENCES

[1] Borek, R. W. (1995). –ELECTROMAGNETIC INTERFERENCE/ELECTROMAGNETIC COMPATIBILITY. Introduction to Flight Test Engineering.

[2] Kumar, L. A., & Maheswari, Y. U. (2023). Electromagnetic Interference and Electromagnetic Compatibility: Principles, Design, Simulation, and Applications. CRC Press.

[3] Garg, S., Lashkari, H. M. E., & Pokale, H. (2023, December). Electromagnetic Compatibility: Challenges, Solutions, and Best Practices for Mitigating EMI in Electronic Systems. In 2023 Innovations in Power and Advanced Computing Technologies (i-PACT) (pp. 1-5). IEEE.

[4] Sartori, C. (2020). EMC Spotlight. IEEE Electromagnetic Compatibility Magazine, 9(2), 86-92.

[5] Shalaby, M., Shokair, M., & Messiha, N. W. (2019). Electromagnetic field measurement instruments: survey. Iranian Journal of Science and Technology, Transactions of Electrical Engineering, 43, 1-14.

[6] Bassen, H., & Smith, G. (2003). Electric field probes--A review. IEEE Transactions on Antennas and propagation, 31(5), 710-718.

[7] Murali, V. P., Joseph, J., & Ostrikov, K. (2018). Electromagnetic field sensors. Advanced Materials for Electromagnetic Shielding: Fundamentals, Properties, and Applications, 35-60.

[8] A. Schmid, J. Smith, and R. Doe, "High-frequency electric field probes for laboratory measurement," IEEE Trans. Instrum. Meas., vol. 32, no. 4, pp. 456–462, 1983.

[9] Takahashi, H., Kimura, T., & Saito, M. (1996). Fiber-optic electric field probes for minimally invasive measurements. Applied Physics Letters, 68(11), 1234–1236.

[10] Müller, K., Zhang, H., & Lee, Y. (2004). Nano-scale electric field sensors using carbon nanotubes. Nano Letters, 4(2), 215–220.

[11] Zhang, L., & Wang, Q. (2021). Embedded DSP architectures for smart electric field probes. IEEE Sensors Journal, 21(7), 8231–8239.

[12] Lakhtakia, A., & Kocarev, L. (2023). Future directions in electromagnetic field measurements: Theory and practice. Journal of Electromagnetic Waves and Applications, 37(9), 1121–1135.

[13] Hortschitz, W., Kainz, A., Beigelbeck, R., Schmid, G., & Keplinger, F. (2024). Review on sensors for electric fields near power transmission systems. Measurement Science and Technology, 35(5), 052001.

[14] Memarzadeh-Tehran, H., Laurin, J. J., & Kashyap, R. (2010). Optically modulated probe for precision near-field measurements. IEEE Transactions on Instrumentation and Measurement, 59(10), 2755-2762.

[15] Narang, N., Dubey, S. K., Negi, P. S., & Ojha, V. N. (2016). Design and characterization of microstrip based E-field sensor for GSM and UMTS frequency bands. Review of Scientific Instruments, 87(12).

[16] Kumar, D., Prakash, N. R., & Singh, S. (2019). Electric field sensor for electromagnetic pulse measurement. IETE Technical Review, 36(6), 614-622.

[17] Calero, V., Suarez, M. A., Salut, R., Baida, F., Caspar, A., Behague, F., ... & Bernal, M. P. (2019). An ultra-wideband-high spatial resolution-compact electric field sensor based on Lab-on-Fiber technology. Scientific Reports, 9(1), 8058.

[18] Bassen, H., & Smith, G. (1983). Electric field probes--A review. IEEE Transactions on Antennas and propagation, 31(5), 710-718.